

A dipole amplifier for electric dipole moments, axion-like particles and a dense dark matter hairs detector

Gary Prézeau¹

¹*Jet Propulsion Laboratory, California Institute of Technology,
4800 Oak Grove Dr, Pasadena, CA 91109, USA*

A tool that can constrain, in minutes, beyond-the-standard-model parameters like electric dipole moments (EDM) down to a lower-bound $d_e^N < 10^{-37} \text{e} \cdot \text{cm}$ in bulk materials, or the coupling of axion-like particles (ALP) to photons down to $|G_{a\gamma\gamma}| < 10^{-16} \text{GeV}^{-1}$, is described. Best limits are $d_e^N < 3 \cdot 10^{-26} \text{e} \cdot \text{cm}$ for neutron EDM and $|G_{a\gamma\gamma}| < 6.6 \cdot 10^{-11} \text{GeV}^{-1}$. The *dipole amplifier* is built from a superconducting loop immersed in a toroidal magnetic field, \vec{B} . When nuclear magnetic moments in the London penetration depth align with \vec{B} , the bulk magnetization is always accompanied by an EDM-induced bulk electric field $\vec{E} \propto \vec{B}$ that generates detectable oscillatory supercurrents with a characteristic frequency $\omega_D \propto d_e^N$. Cold dark matter (CDM) ALP are formally similar where $\omega_D \propto |G_{a\gamma\gamma}| \sqrt{n_a}/(2m_a)$ with m_a the ALP mass and n_a its number density. A space probe traversing a dark matter hair with a dipole amplifier is sensitive enough to detect ALP density variations if $|G_{a\gamma\gamma}| \sqrt{n_h}/(2m_a) > 4.9 \cdot 10^{-27}$ where n_h is the ALP number density in the hair.

PACS numbers: 11.30.Er, 95.35.+d, 14.80.Va, 32.10.Dk

Experimental searches for the axion and the neutron EDM have been ongoing for decades, motivated by what they could reveal about physics beyond the standard model [1, 2]. Indeed, the axion is a particle thought to have been created when the universe was as young as 10^{-29} s; it was originally proposed to explain the *strong CP problem*, by which the neutron EDM appears to be infinitesimal despite the CP-violating terms in the QCD Lagrangian. Its link to QCD and its appearance early in the universe made the axion a popular CDM candidate.

Consider an effective Lagrangian for CDM ALP, an external electromagnetic field, and an atom in a bulk material that includes P-odd/T-odd (\mathcal{PT}) interactions

$$\begin{aligned} \mathcal{L}_{\text{eff}} = & \mathcal{L}_{\text{K.E.}} - \frac{1}{4\mu_0} F_{\mu\nu} F^{\mu\nu} - A_\mu J_{\text{free}}^\mu + \frac{1}{2} F_{\mu\nu} M^{\mu\nu} \\ & + \left[V_{\text{ES}} + V_{Ne} + V_{NN} + \frac{d_e^p \bar{\psi}_p i \sigma^{\mu\nu} \gamma_5 \psi_p}{2 \mu_p} c F_{\mu\nu} \right] \\ & - \frac{G_{a\gamma\gamma}^i a_i}{4} \frac{F_{\mu\nu} \tilde{F}^{\mu\nu}}{\mu_0}, \end{aligned} \quad (1)$$

where $\mathcal{L}_{\text{K.E.}}$ contains the kinetic energy terms, V_{ES} is the atomic electrostatic potential energy, V_{Ne} has \mathcal{PT} nucleon-electron interactions, V_{NN} represents the nuclear potential energy including \mathcal{PT} NN interactions, a_i is an ALP field, $G_{a\gamma\gamma}^i$ is an ALP coupling constant to photons, d_e^p is the electric dipole moment of field $p = \text{e,p,n}$, ψ_p is the wave function of the field p , and μ_p its magnetic moment; the sums over i and p are implicit. A_μ is the photon field, J_{free}^μ represents the free current density, $\tilde{F}^{\mu\nu} = \epsilon^{\alpha\beta\mu\nu} F_{\alpha\beta}$ is the dual electromagnetic tensor, and the material's magnetization-polarization tensor (MPT) is given by $M^{0i} = cP^i$, $M^{ij} = -\epsilon^{ijk} M^k$ and $M^{\mu\nu} = -M^{\nu\mu}$ with \vec{P} the bulk electric polarization and \vec{M} the bulk magnetization of the material.

The \mathcal{PT} interactions manifest themselves differently

depending on whether an atom is paramagnetic or diamagnetic. Following the arguments in Refs. [3] in the case of a diamagnetic atom like ^{199}Hg , and neglecting the electron EDM, the multipole expansion of V_{ES} leads to a cancellation of the EDM terms in the brackets to leading-order. The non-zero terms are higher multipoles such as the Schiff moments. The \mathcal{PT} moments are $\propto \mu_s d_e^N \vec{I}$ where \vec{I} is the angular momentum of the nucleus, d_e^N is the nuclear EDM suppressed by μ_s , a small dimensionless factor representing the screening of d_e^N by the electron cloud. Depending on the atom, Schiff moments can be very difficult to calculate and we parameterize the EDM suppression with the order-of-magnitude formula $\mu_s \sim 10Z^2 r_{\text{atom}}^2 / r_{\text{nuc}}^2$ where r_{atom} is the atomic radius, r_{nuc} is the nuclear charge radius and Z the atomic number; this is conservative since it doesn't account for potential octopole enhancements. Screening differences between vaporized atoms and solids are not considered. The bracketed \mathcal{PT} contributions of the second line in Eq. (1) can be replaced by

$$\sum_{\alpha=\text{ES}, Ne, NN} V_\alpha + \frac{d_e^p \bar{\psi}_p i \sigma^{\mu\nu} \gamma_5 \psi_p}{2\mu_p} c F_{\mu\nu} \doteq \frac{\mu_s d_e^N \bar{\psi} i \sigma^{\mu\nu} \gamma_5 \psi}{2\mu_N} c F_{\mu\nu} \quad (2)$$

where ψ is the nuclear wave function and μ_N is the nuclear magnetic moment. Keeping only the ALP + \mathcal{PT} + electromagnetic terms, Eq. (1) becomes

$$\mathcal{L}_{\text{eff}} \doteq -\frac{1}{4\mu_0} F_{\mu\nu} F^{\mu\nu} - A_\mu J_{\text{free}}^\mu + \frac{1}{2} F_{\mu\nu} \tilde{M}^{\mu\nu} \quad (3)$$

$$\tilde{M}^{\mu\nu} = M^{\mu\nu} - \frac{G_{a\gamma\gamma}^i a_i \tilde{F}^{\mu\nu}}{2 \mu_0} + c \frac{\mu_s d_e^N \bar{\psi} i \sigma^{\mu\nu} \gamma_5 \psi}{\mu_N} \quad (4)$$

The Euler-Lagrange equations can now be applied to Eq. (3) to extract the Maxwell equations (ME)

$$\partial_\mu \tilde{F}^{\mu\nu} = 0 \quad (5)$$

$$\partial_\mu (F^{\mu\nu} - \mu_0 \tilde{M}^{\mu\nu}) = \mu_0 J_{\text{free}}^\mu \quad (6)$$

Below, we first solve the ME in an insulator immersed in a magnetic field with $J_{\text{free}}^\mu = 0$, and show that although an electric field is generated, it is too faint to be measured easily. This is followed by the solutions of the ME in the dipole amplifier, found to be oscillatory with a frequency proportional to the nuclear EDM's. In the case of a generic ALP a , the frequency will be seen to be proportional to $G_{a\gamma\gamma}$, its coupling to photons, times the square root of the ALP number density n_a divided by its mass m_a . In the presence of a CDM ALP background, detection of dark matter *hairs* [4] (long, dense, filaments of CDM spreading outward from planets) using a dipole amplifier is shown to be feasible.

EDM: INSULATOR. We begin by solving ME when $J_{\text{free}}^\mu = 0$ to clarify the conditions under which an EDM-induced electric field can be detected in that case.

In a bulk material, a nuclear electric dipole moment will be either parallel or anti-parallel to its magnetic moment. If a powerful magnetic field \vec{B} polarizes a substantial fraction of the nuclei in a material, the nuclear EDM is also amplified thanks to the appearance of a macroscopic electric field $\propto \langle \vec{\sigma} \rangle$, the average magnetic polarization of the bulk material. Since, $\langle \vec{\sigma} \rangle \propto \vec{H}$, it follows that $\vec{E} \propto \vec{H}$. Indeed, consider Eq. (6) for F^{i0}

$$\partial^i \left(E^i - c\mu_0 \tilde{M}^{i0} \right) = 0. \quad (7)$$

The non-relativistic limit of \tilde{M}^{i0} (ignoring ALP treated below)

$$\tilde{M}^{i0} = -cP^i + c \frac{\mu_s d_e^N \bar{\psi} i \sigma^{i0} \gamma_5 \psi}{\mu_N} \\ c \frac{\mu_s d_e^N \bar{\psi} i \sigma^{i0} \gamma_5 \psi}{\mu_N} \rightarrow -c\mu_s \frac{d_e^N}{\mu_N} \langle \sigma^i \rangle_N = -c\mu_s \frac{d_e^N}{\mu_N} \chi_{\mathcal{N}}(T) H^i \quad (8)$$

where $\chi_{\mathcal{N}}(T)$ is the temperature-dependent nuclear magnetic susceptibility of the insulator, $\langle \sigma^i \rangle_N$ is the average nuclear magnetization, and H^i is the corresponding magnetic field strength. Since the electric polarizability of insulators is generally small and proportional to the EDM-induced electric field, we can neglect the \vec{P} contribution. The ME in the insulator are now

$$\vec{\nabla} \cdot \vec{B} = 0 \quad (9)$$

$$\vec{\nabla} \times \vec{E} + \frac{\partial \vec{B}}{\partial t} = 0 \quad (10)$$

$$\vec{\nabla} \cdot \left(\vec{E} + \frac{c^2 \mu_0}{\mu_N} d_e^N \mu_s \chi_{\mathcal{N}}(T) \vec{H} \right) = 0 \quad (11)$$

$$\vec{\nabla} \times \vec{H} - \epsilon_0 \frac{\partial}{\partial t} \left(\vec{E} + \frac{c^2 \mu_0}{\mu_N} d_e^N \mu_s \chi_{\mathcal{N}}(T) \vec{H} \right) = 0 \quad (12)$$

We can write down a solution to the ME from Eq. (11):

$$\vec{E} = -\frac{c^2 \mu_0}{\mu_N} d_e^N \mu_s \chi_{\mathcal{N}}(T) \vec{H}. \quad (13)$$

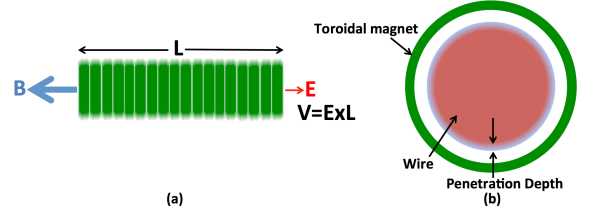


FIG. 1: Graph (a) shows a solenoid immersing an insulator in a magnetic field \vec{B} . An electric field \vec{E} is generated aligned with \vec{B} . Graph (b) shows a cross-section of a dipole amplifier: a toroidal magnet immersing a superconducting loop in a magnetic field. A supercurrent aligned with the magnetic field is generated by the wire material's nuclear EDM, or a background ALP, within the penetration depth λ_L .

Assuming $\chi_{\mathcal{N}}(T)$ to be spatially uniform in the insulator, the fields are seen to be static using $\vec{\nabla} \times \vec{E} \propto \vec{\nabla} \times \vec{H} = 0$ in Eq. (10). Assuming that the EDM of the material stems entirely from the nucleus which acts like an ideal paramagnetic, we can rewrite $\chi_{\mathcal{N}}(T) \vec{H}$

$$\vec{E} = -c^2 \mu_0 d_e^N \mu_s N B_I(x) \langle \hat{\sigma} \rangle_{\mathcal{N}}, \quad (14)$$

$$B_I(x) \equiv \frac{2I+1}{2I} \tanh\left(\frac{2I+1}{2I}x\right) - \frac{1}{2I} \tanh\left(\frac{x}{2I}\right) \quad (15)$$

where $x \equiv \mu_N \vec{B} / (k_B T)$, $\langle \hat{\sigma} \rangle_{\mathcal{N}}$ is the average nuclear magnetization direction, N is the number of nuclei per unit volume and I is the nuclear spin. To get a sense of the magnitude of that electric field, consider the case of ^{127}I with parameters given in Tab. I: $|E| = 3.9 \cdot 10^{-14}$ V/m for $d_e^N \sim 10^{-28}$ e·cm. A solenoid coiled around an iodine wire (Fig. 1a) requires $L = 2.5 \cdot 10^4$ m for a detection on a nanovoltmeter. For iodine, this may be too conservative because of its relatively large nuclear spin (and, perhaps, the atomic enhancements of the unpaired electron EDM [2]), but the dipole amplifier described next is far more sensitive and the main topic of this letter.

EDM: DIPOLE AMPLIFIER. The dipole amplifier can easily measure a $d_e^N \sim 10^{-31}$ e·cm. It is composed of a superconducting wire inside a toroidal magnet (Fig. 1b). The physics behind the amplifier is intuitive: if a bulk material, with a nuclear magnetic moment, immersed in a magnetic field generates an electric field given by Eq. (13), immersing a superconducting loop in a toroidal magnetic field will generate a current, increasing with time, within the penetration depth of that superconducting loop. Measuring that current will therefore provide a direct measurement of the nuclear EDM of the superconducting material. Note that the magnetic field magnitude must be less than the critical field of the superconductor, B_c . Nuclear EDM experiments in atoms like vaporized ^{199}Hg have a relatively low $B_c \sim 4.1 \cdot 10^{-2}$ T. Since magnetic fields radially decay exponentially inside a superconducting wire, the weak field approximation of

Eq. (14), Curie's law, will be used to solve ME

$$\vec{E} = -c^2 \mu_0 d_e^N \mu_s \frac{(I+1) N \mu_N \vec{B}}{I 3 k_B T}. \quad (16)$$

with the constraint $\mu_N \vec{B} \ll k_B T$. In the case of ^{199}Hg with a $\mu_N = 0.88 \mu_N$ and $|\vec{B}| \sim 10^{-2}$ T, this corresponds to the weak constraint $T \gg 10^{-5}$ K.

The ME describing the dipole amplifier are the same as above except for a free current density, $J_{\text{free}}^\mu = (0, \vec{J})$, on the rhs of Eq. (12). Eq. (16) is the solution of Eq. (11) and only Eq. (9), Eq. (10) and Eq. (12) (with \vec{J} on the rhs) need to be solved. Let \vec{B} satisfying Eq. (9) be parametrized by B_l and B_ϕ

$$\vec{B} = e^{-(R_w - \rho)/\lambda_L} B_0 (B_l \hat{l} + B_\phi \hat{\phi}), \quad \vec{\nabla} \cdot \vec{B} = 0, \quad (17)$$

where R_w is the radius of the wire, ρ is the radial coordinate from the center of the wire, \hat{l} is the wire direction, $\hat{\phi}$ is the azimuthal direction and λ_L is the London penetration depth. At time $t = 0$, we expect $B_l = 1$ and $B_\phi = 0$. Neglecting the magnetization $\vec{M} \ll \vec{B}/\mu_0$, the equations to solve and their solutions are

$$\vec{\nabla} \times \vec{E} + \frac{\partial \vec{B}}{\partial t} = 0 \quad (18)$$

$$\vec{\nabla} \times \vec{B} = \mu_0 \vec{J} \quad (19)$$

$$B_l = \cos(\omega_D t) \quad (20)$$

$$B_\phi = -\sin(\omega_D t) \quad (21)$$

$$\omega_D \equiv c^2 \mu_0 \frac{\mu_s d_e^N}{\lambda_L} \frac{(I+1) N \mu_N}{I 3 k_B T} \quad (22)$$

$$\vec{J} = \frac{e^{-(R-\rho)/\lambda_L} B_0}{\lambda_L \mu_0} (B_\phi \hat{l} - B_l \hat{\phi}) \quad (23)$$

These solutions satisfy the London Equations. They also feature a characteristic timescale $|\omega_D|^{-1}$ during which the magnetic field and supercurrents in the penetration depth oscillate between their \hat{l} and $\hat{\phi}$ components. Substituting in parameters for ^{199}Hg (Tab. I) in ω_D assuming a standard model value $d_e^N = 10^{-31}$ e·cm, we obtain $T|\omega_D| = 4.6 \cdot 10^{-12}$ K·Hz. At $T = 1$ K, this corresponds to a period of 7000 years so that an experiment would need to run at $T \sim 10^{-4}$ K to see a full oscillation of the fields and currents in the superconductor. Although seeing the full oscillation would likely yield the most accurate results, observing a linear rise of a \hat{l} -component supercurrent for small $\omega_D t$ gives fast results and sensitivity to $d_e^N \ll 10^{-31}$. For $|\omega_D|t \ll 1$, $B_\phi \cong -\omega_D t$

$$\lim_{\omega_D t \ll 1} J_l = -e^{-(R-\rho)/\lambda_L} \frac{B_0 \omega_D t}{\mu_0 \lambda_L} \quad (24)$$

for which the l -component of the current density $J_l \propto \lambda_L^{-2} \propto n_e$ the charge carrier density. Integrating Eq. (24) over ρ and ϕ to obtain the current magnitude j_l ,

$$j_l = \frac{2\pi R_w B_0}{\mu_0} |\omega_D| t. \quad (25)$$

	λ_L (Å)	μ_N (μ_N)	N (m^{-3})	μ_s	I	R_w (cm)	B_0 (T)
^{127}I	N/A	3.3	$2.3 \cdot 10^{28}$	10^{-4}	5/2	N/A	$k_B T / \mu_N$
^{199}Hg	520	0.88	$4 \cdot 10^{28}$	10^{-3}	1/2	1	10^{-2}
^{208}Pb	370	0	N/A	N/A	0	1	10^{-2}

TABLE I: Bulk and experimental parameters.

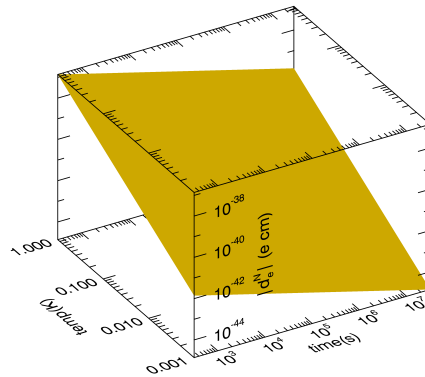


FIG. 2: Detectability of ^{199}Hg nuclear EDM as a function of time and temperature for an experimental setup capable of detecting a 1 pA current. The parameters used are given in Tab. I. The smallest $|d_e^N|$ detectable after one year at $T = 10^{-3}$ K is $|d_e^N| \sim 10^{-45}$ e·cm. After 315 s, an experiment running at 1 K is already sensitive to $|d_e^N| \sim 10^{-37}$ e·cm. Current limits on neutron EDM are $\sim 3 \cdot 10^{-26}$ e·cm projected to reach 10^{-28} e·cm at best.

Consider an experiment sensitive to $j_l \sim 1$ pA (e.g. by inserting a Josephson Junction in the loop or measuring the rising B_ϕ -field) with ^{199}Hg parameters from Tab. I. Putting $j_l = 10^{-12}$ A in Eq. (25), Fig. 2 plots $|d_e^N|$ as a function of time and temperature showing detectability levels for $10^{-3} < T(K) < 1$ within a year. Fig. 2 shows that a dipole amplifier is sensitive to nuclear EDM down to $|d_e^N| \sim 10^{-45}$ e·cm at $T = 10^{-3}$ K over a year, while a $|d_e^N| \sim 10^{-37}$ e·cm can be measured in 5 minutes at $T = 1$ K. That exceptional sensitivity implies that superconducting materials with smaller μ_s than ^{199}Hg can be used if the nuclear matrix elements are more easily calculable than the soft nucleus of ^{199}Hg .

AXION-LIKE PARTICLES. Observational and laboratory constraints on the axion have typically relied on detecting or constraining on-shell photons generated by the Primakoff effect. As the amplifier relies on measuring a DC electric field induced by a background ALP field, the final photon 4-momentum does not generally satisfy $q^2 = 0$ expanding the final photon phase space by orders of magnitude: combined with the sensitivity of superconductors to infinitesimal electric fields, this explains why the dipole amplifier is so sensitive compared to other ap-

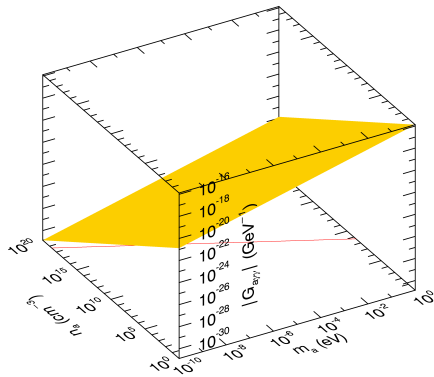


FIG. 3: A plot of the CDM ALP parameter space explored by the dipole amplifier sensitive to $j_i \sim 1$ pA. The entire region above the yellow plane would be explored in 60 s which corresponds to all $|G_{a\gamma\gamma}| > 10^{-16}$ GeV $^{-1}$ for $m_a < 1$ eV and $n_a > 1$ cm $^{-3}$, greater than the parameter space considered in Ref. [5]. The red line corresponds to the local CDM limit [5] $n_a m_a = 0.45$ GeV/cm 3 while the lower-bound from horizontal branch stars ($|G_{a\gamma\gamma}| < 6.6 \cdot 10^{-11}$ GeV $^{-1}$ [6]) is much larger.

proaches. For a CDM ALP background, ω_D is given by

$$\omega_D = \frac{|G_{a\gamma\gamma}^i| a_i}{2} \frac{c}{\lambda_L(T)}. \quad (26)$$

The a_i are constrained by the covariant normalization condition $\int a_i^2 2m_{a_i} dV = n_i$ where there are n_i CDM ALP of type i in volume V . For uniform ALP densities, the total number N of CDM ALP in volume V is

$$\sum_i 2m_{a_i} a_i^2 = \frac{N}{V} \equiv n_a \xrightarrow{\text{single species}} a = \sqrt{\frac{n_a}{2m_a}}. \quad (27)$$

Consider an experiment that runs for 1 minute with a dipole amplifier sensitive to 1 pA currents, and a CDM ALP background composed of a generic species a . To suppress a signal from nuclear EDM, choose a diamagnetic superconducting material with a null nuclear spin like ^{208}Pb . Detecting a $j_l > 1$ pA in 1 minute requires

$$|G_{a\gamma\gamma}| \sqrt{\frac{n_a}{2m_a}} > \frac{2\lambda_L (10^{-12}\text{A})\mu_0}{c60\text{s} \ 2\pi R_w B_0}. \quad (28)$$

For ^{208}Pb and Tab. I values, the sensitivity of the dipole amplifier is plotted in Fig. 3 where it is seen that within a minute, the entire parameter space $|G_{a\gamma\gamma}| > 10^{-16}$ GeV $^{-1}$ for $m_a < 1$ eV and $n_a > 1$ cm $^{-3}$ is explored. Some of that parameter space is already constrained by astrophysical sources such as limits stemming from horizontal branch stars ($|G_{a\gamma\gamma}| < 6.6 \cdot 10^{-11}$ GeV $^{-1}$) [6] and a local CDM density of $n_a m_a = 0.45$ GeV/cm 3 assuming all CDM to be ALP.

We will consider the case of relativistic ALP, and methods to disentangle their signal in a dipole amplifier from CDM ALP, in a future paper.

DENSE DARK MATTER HAIRS. The dipole amplifier could also be used to detect dark matter hairs [4] if CDM ALP are found to exist: assuming a probe passes through a 1 m wide hair in 10^{-4} s, a detectable pA current spike could be detected as long as

$$|G_{a\gamma\gamma}| \sqrt{\frac{n_h}{(2m_a)}} > 4.9 \cdot 10^{-27} \quad (29)$$

where n_h is the hair ALP number density. As a reference point, consider typical values often used for axions [5]: if $n_a \sim 10^{13}$ /cm 3 , $m_a \sim 10^{-5}$ eV and $G_{a\gamma\gamma} \sim 10^{-12}$ /GeV, $|G_{a\gamma\gamma}| \sqrt{n_a/(2m_a)} = 6.2 \cdot 10^{-20}$. As discussed in [4], hairs are potential sources of unique data sets of the fine-grained dark matter streams criss-crossing the solar system, including their velocity and density distributions. This data, unobtainable any other way, is highly relevant for structure formation and cosmology and would act as a constraint on simulations of halo formation [7]. In addition, hairs contain radial density tomographic data of the planets and moons from which they spread out, providing information that could be used to better understand planetary formation and the history of the solar system.

The author is grateful to Brad Plaster and Takeyasu Ito for useful comments and suggestions. The research was carried out at the Jet Propulsion Laboratory, California Institute of Technology, under a contract with the National Aeronautics and Space Administration. ©2016 California Institute of Technology. Government sponsorship acknowledged.

-
- [1] R. D. Peccei and H. R. Quinn, Phys. Rev. D **16**, 1791 (1977). doi:10.1103/PhysRevD.16.1791
 - [2] M. Pospelov and A. Ritz, Annals Phys. **318**, 119 (2005) doi:10.1016/j.aop.2005.04.002 [hep-ph/0504231].
 - [3] V. Spevak, N. Auerbach and V. V. Flambaum, Phys. Rev. C **56**, 1357 (1997) doi:10.1103/PhysRevC.56.1357 [nucl-th/9612044].
 - [4] G. Pr ezeau, Astrophys. J. **814**, no. 2, 122 (2015) doi:10.1088/0004-637X/814/2/122 [arXiv:1507.07009 [astro-ph.CO]].
 - [5] K. A. Olive *et al.* [Particle Data Group Collaboration], *Axions and other similar particles* Chin. Phys. C **38**, 090001 (2014). doi:10.1088/1674-1137/38/9/090001
 - [6] A. Ayala, I. Dom nguez, M. Giannotti, A. Mirizzi and O. Straniero, Phys. Rev. Lett. **113**, no. 19, 191302 (2014) doi:10.1103/PhysRevLett.113.191302 [arXiv:1406.6053 [astro-ph.SR]].
 - [7] M. Vogelsberger and S. D. M. White, Mon. Not. Roy. Astron. Soc. **413**, 1419 (2011) doi:10.1111/j.1365-2966.2011.18224.x [arXiv:1002.3162 [astro-ph.CO]].